International Journal of Microwave and Wireless Technologies

cambridge.org/mrf

Joint phase shift and time delay to reduce beam splitting effect on reflecting intelligent surface

Hiba A. Alsawaf[1,2] and Saad Ahmed Ayoob[2]

[1]Department of Electronic Engineering, Electronics Engineering, Ninevah University, Mosul, Iraq and [2]Electrical Engineering Department, College of Engineering, University of Mosul, Mosul, Iraq

Research Paper

Cite this article: Alsawaf HA, Ayoob SA (2025) Joint phase shift and time delay to reduce beam splitting effect on reflecting intelligent surface. *International Journal of Microwave and Wireless Technologies* **17**(4), 582–594. https://doi.org/10.1017/S1759078725101669

Received: 3 September 2024
Revised: 7 May 2025
Accepted: 12 May 2025

Keywords:
IRS; mm-wave; phase shifting and effect of beam splitting

Corresponding author: Hiba A. Alsawaf;
Email: hiba.hmdoon@uoninevah.edu.iq

Abstract

Intelligent Reflecting Surface (IRS) technology operating at mm-wave frequencies is promising for 6G applications. However, this technique faces the challenge of beam splitting, as beams cannot be directed accurately at all frequencies. To enhance system performance and lessen the beam spillting effect, the IRS is developed using phase shifters and time delay modules, as the problem is analyzed in this paper. The results of the simulation revealed that the proposed system, which is based on sub-surface IRS and time delay modules, successfully overcomes the packet splitting challenge effectively. The proposed architecture was 94.5% better in gain compared with the traditional architecture. The results explained a 54% improvement in data rate when time delay is used in the Phase-shift-Time delay-Phase delay (PTDP) system compared to the conventional design. Moreover, the use of 2-bit phase shifting alone in the proposed design was appropriate to realize close to optimal performance due to the system capability to direct power in the desired direction through the use of precoding technology, which compensates for losses resulting from beam splitting.

Introduction

Millimeter wave (mm-wave) technologies are among the most promising technologies for wireless systems beyond 5G and 6G thanks to their ability to take advantage of abundant unused spectrum resources [1, 2]. Millimeter waves have the advantage of high bandwidth but suffer from poor propagation in real environments due to large signal loss and easy blockage [3–5]. Compared to frequencies below 6 GHz, mm wave frequencies are easier to block through higher Directivity. IRSs (Intelligent Reflecting Surfaces) have been an inexpensive and cost-effective solution to this problem. IRS stands for a smart surface that is capable of intelligently reflecting radio waves through phase control of waves while interacting with its surface [6]. Because IRS is used in mm-wave communications, it is a perfect technology for networks that will be 5G and beyond [7]. The RIS (Reconfigurable Intelligent Surface) technology has attracted lots of attention of late, and the current paper was focused on areas such as precoding design [8, 9], channel estimation [10, 11], and architectural design [12], with major interest being in narrowband applications. Consider RIS technique has already been employed with excellent success to various communications systems for improving the user's reception quality of the received signal [9]. A greater weighted sum rate was achieved with a block coordinate descent algorithm to optimize the parameters of base stations and RIS separately and thus enhance system performance [13]. Substantial research has been conducted to examine the prospective uses of RIS technology in broadband communication systems, particularly in mm-wave frequency bands [14–18]. The authors demonstrated the effectiveness of using RIS-aided hybrid relay networks in mm-wave communication systems, particularly when combined with advanced machine learning techniques [19]. The use of conventional beamforming methods in large IRS mm-wave deployments results in undesirable scattering of beams across a variety of frequency and angular spaces. This phenomenon is known as beam splitting, and it represents a greater challenge in mm-wave communications than beam squint [16, 20–23]. In the study by Chen *et al.* [16], the authors used channel covariance matrix and long-range angle information to develop a technique aimed at improving data transmission rate in environments affected by beam splitting. Although deployment of distributed IRSs will reduce the problem of beam splitting to a large extent, it renders a high loss in received signal strength since elements constituting the surface are quite small. In addition, all the methods proposed in study by Chen *et al.* [16] rely on precoding techniques that are invariant across frequencies. In paper by Li *et al.* [24], the authors presented scientific inputs to the immense potential of remote sensing systems in enhancing mm-wave communication and sensing systems by optimizing the key parameters such as beam scanning, beam splitting, and performance evaluation techniques accurately. The study [25] presented two new designs of a simultaneous transmit and receive RIS (STAR-RIS) for application

© The Author(s), 2025. Published by Cambridge University Press in association with The European Microwave Association.

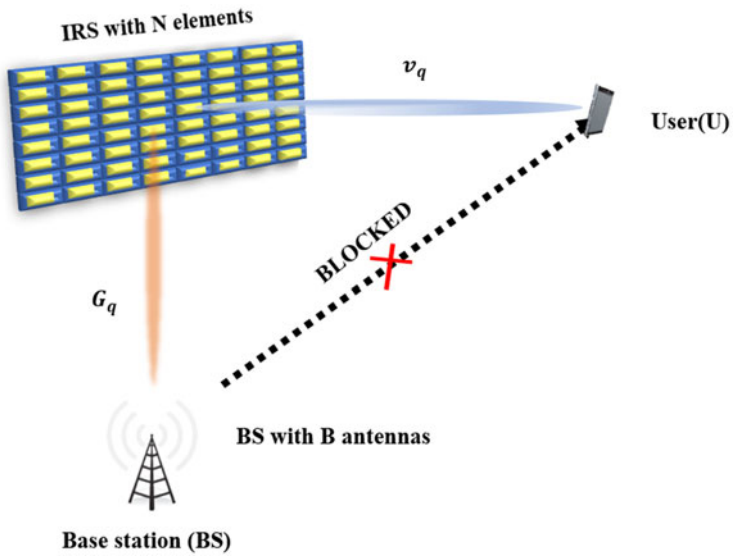


Figure 1. The IRS-assisted mm-wave technique.

in terahertz (THz) communication systems. These two designs have been suggestedto mitigate the beam splitting effects, which is a major challenge in high-frequency communication systems.

The proposed approach addresses the beam-split effect and ensures beam alignment across all frequencies, focusing on a wideband-specific design that considers frequency dispersion in mm-wave channels. Unlike previous studies that treat IRS and precoding separately, leading to suboptimal performance, this approach jointly designs IRS and precoding for improved performance. The system optimizes signal routing using IRS to mitigate path loss effectively. Moreover, it focuses on computational efficiency for large systems with a high number of IRS elements and sub-frequencies, which has not been satisfactorily addressed before.

The proposed solution addresses this problem through low-complexity algorithms that work efficiently with large-scale systems.

This paper contributes to mitigating the effect of beam split in IRS. A sublayered IRS architecture with fewer time delay (TD) units is proposed. The subarray element is composed of a cascaded connection of two-phase shifters and a shared time delay module. The elements receive and process the signal sequentially, with the signal passing through first phase shifter, the TD unit, and then the second phase shifter. This setup permits a transition from traditional narrowband precoding, which relies solely on phase, to wideband precoding based on a combination of TD and phase shift, leading to an enhanced tradeoff between data rate, device cost, and power dissipation.

A wideband frequency-dependent precoder design is presented based on the sub-connected architecture. This design aims to constructively generate overlapping signals to be assembled into different receiving elements by controlling the phases of the first layer of the subarray. The beam must be directed towards the carrier frequency to the receiving end by the second layer. For each sub-carrier, the common time delay unit aligns it so that the produced beams precisely match the desired physical direction.

The remainder of this paper is structured as: Section 2 introduces a comprehensive model of the system and signal. Section 3 discusses the effect of beam splitting on the IRS, while Section 4 presents the proposed IRS architecture along with its design analysis. The outcome and simulation will be explained in Section 5, and Section 6 summarizes the paper.

Notations: Bold letters represent mathematical quantities, where uppercase letters indicate matrices and lowercase letters indicate vectors.

A^T: The matrix is created by interchanging the rows and columns of matrix A.

A^H: The matrix is created by applying the conjugate operation to the elements in the matrix A^T.

$|a|$: The vector length a.

$\mathbb{E}[Z]$: The average expected value of the random variable Z.

$U(a, b)$: Probability Distribution in which each value between b and a has equal likelihood.

$\otimes$: Kronecker multiplication is a special multiplication of two matrices.

$\odot$: Hadamard multiplication, Another unique matrix multiplication operation between two matrices,

diag(a): a diagonal matrix with the vector elements on the main diagonal

System and signal model

This paper investigates mm-wave communication with an IRS, as indicated in Fig. 1. Specifically, it examines a system in which a BS equipped with a uniform linear array (ULA) of antennas (B) employs an IRS to transmit signals to a single user. While the model can be generalized to the multi-user scenario, a single-user model is adopted for simplicity. The IRS is a uniform planar array (UPA) and consists of N IRS elements which are equal to N_1N_2 where $N_1$and N_1 represent the IRS elements in the horizontal and vertical direction, respectively. The sub-carriers (Q) in orthogonal frequency division multiplexing (OFDM) technology are utilized to modulate the user signals and mitigate wideband channel dispersion. The IRS is positioned in the x–y plane, with the BS at (0,0), the IRS at (0, 25 m), and the user at (25 m, 25 m).

The received signal at qth subcarrier is given [16]:

$$y_q = (v_q^T \Theta G_q + h_q)x_q + n_q$$
$$y_q = v_q^T \Theta G_q x_q + n_q \quad (1)$$

https://doi.org/10.1017/S1759078725101669 Published online by Cambridge University Press

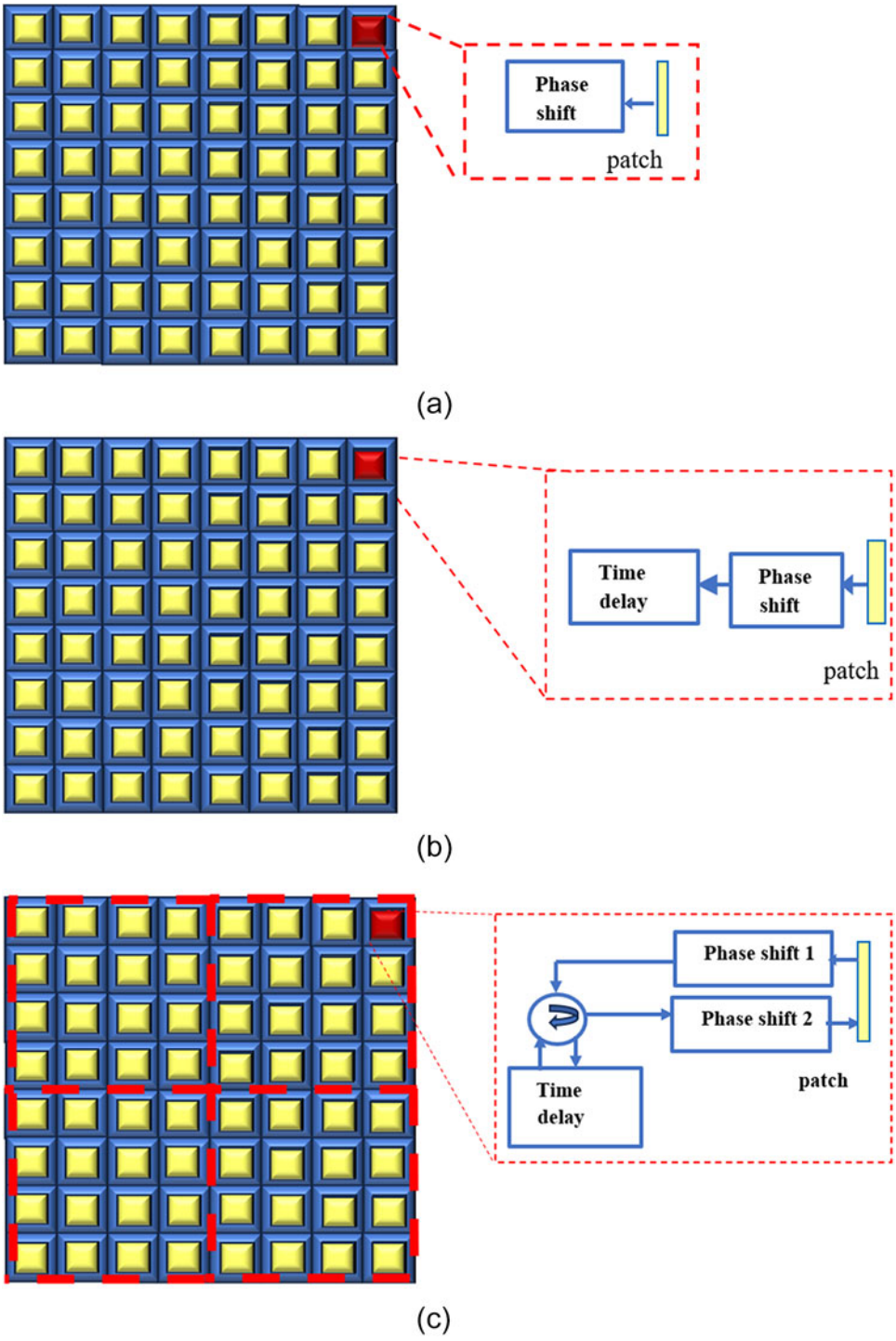


Figure 2. IRS architecture: (a) traditional IRS (B) IRS with TD and phase shift (c) proposed PTDP.

h_q : the direct channel from BS to user,which is blocked, v_q: the channel from IRS to user, $v_q^T = [v_{q,1},]$

$$\Theta = diag\,(\theta) = diag\,(e^{j\theta_1}, e^{j\theta_2}, \ \ldots\ldots, e^{j\theta_N}) \tag{2}$$

The IRS phase shift matrix (Θ) is diagonal,which each diagonal entry $e^{j\theta_N}$ corresponds to a phase shift introduced by the n^{th} IRS element [26]. Each element in IRS adjusts the phase of the incoming signal to maximize the constructive alignment of signals at the user. This is key for beamforming or mitigating beam-split effects.

Θ: The IRS reflection coefficient, it was considered that the reflection amplitude at the IRS is constant [7, 27],$G_q \in \mathbb{C}^{N\times B}$: the channel from BS to IRS, $x_q = wr_q \in \mathbb{C}^{B\times 1}$ is the transmitted signal at the BS, $w \in \mathbb{C}^{B\times 1}$ is the precoding vector, at the q^{th} subcarrier, $r_q \in \mathbb{C}$ denoted the information of transmitting, which

https://doi.org/10.1017/S1759078725101669 Published online by Cambridge University Press

Table 1. Applied parameters in the simulation

Parameter	Definition	value
d_1	The separation distance between BS and the IRS	*25 m*
d_2	The separation distance between IRS and U	*25 m*
N	The no. of IRS elements	*64×64*
S	sub-arrays in IRS	*16 ×16*
P	The number of the elemnts in sub-arrays of IRS	*4×4*
Q	Number of subcarriers	*128*
f_c	Carrier frequency	*28 GHz*
f_s	Bandwidth	*2 GHz*
σ^2	Noise power	*−90 dBm*
B	The number of BS antennas	*1*
α_1	Elevation angle of the IRS's angle of arrival	$\frac{\pi}{4}$
β_1	Azimuth angle of the IRS's angle of arrival	$\frac{\pi}{2}$
α_2	The elevation angle of (AoD)	$\frac{\pi}{4}$
β_2	The azimuth angle of (AoD)	0

fulfilled $\mathbb{E}\left[|r|^2\right] = 1$, n_q: presents the Additive White Gaussian Noise (AWGN) with mean = 0,and variance σ^2 [28, 29].

The IRS has a line of sight directly . Thus, the channel of BS-IRS is expressed as [30–32]:

$$G_q = {}_1 e^{-j2\pi f_q t_1} k\, b^H \tag{3}$$

G_q discribed how the signal propagates from the BS to the IRS, accounting for path loss $t_1 \in \mathbb{R}^+$, phase delays $e^{-j2\pi f_q t_1}$, and array response vectors at both ends, $g_1 \in \mathbb{C}$ represented the BS-IRS path gain. The frequency of subcarrier q^{th} is determined according to the following equation [16, 33]:

$$f_q = f_c + \frac{f_s}{Q}\left(q - 1 - \frac{Q-1}{2}\right) \tag{4}$$

f_c: the carrier frequency, f_s: the bandwidth, $d = \frac{\lambda}{2} = \frac{c}{2f_c}$ denoted to the distance between the base station antennas; it also represents the distance between the IRS elements, c denoted speed of light and $q = 1, 2, \ldots, Q$.

$\emptyset$: Symbolized the transmission angle of the BS. α_1 and β_1 represented the elevation and azimuth angles of the direction from which the signal arrives at the IRS. These angles are constrained by the following conditions:$\beta \in U(-\pi, \pi)$, $\alpha \in U\left(0, \frac{\pi}{2}\right)$ and $\emptyset \in \left(-\frac{\pi}{2}, \frac{\pi}{2}\right)$. The BS-IRS path gain is expressed [30]:

$$g_1 = \frac{c}{4\pi f_q d_1} e^{\frac{-\tau d_1}{2}} \approx \frac{c}{4\pi f_q d_1} \tag{5}$$

The term $e^{\frac{-\tau d_1}{2}}$ can often be neglected at mm-wave since molecular absorption is minimal in this frequency range. d_1 represents the distance between the IRS and the Base Station (BS), while τ representing the effect of the molecular absorption.

k is the IRS steering vector with UPA that is defined as [34, 35]:

$$k = \frac{1}{\sqrt{N_1 N_2}}\left[1, \ldots, e^{\frac{j2\pi f_q}{c}(N_1-1)d\sin\alpha_1\cos\beta_1}\right]^T \otimes \left[1, \ldots, e^{\frac{j2\pi f_q}{c}(N_2-1)d\sin\alpha_1\sin\beta_1}\right]^T \tag{6}$$

The steering vector (k) describes the phase shifts applied to each IRS element in order to steer the beam in specific spatial directions (α, β). The terms $e^{\frac{j2\pi f_q}{c}(N_1-1)d\sin\alpha_1\cos\beta_1}$ and $e^{\frac{j2\pi f_q}{c}(N_2-1)d\sin\alpha_1\sin\beta_1}$ represented the difference across elements,determined by the spatial direction (α, β), f_q and number of elements (N_1, N_2) and spacing (d).

b is The base station steering vector with ULA, which is defined as [36]:

$$b = \frac{1}{\sqrt{B}}\left[1, \ldots, e^{\frac{j2\pi f_q}{c}(B-1)d\sin\emptyset}\right]^T \tag{7}$$

B: Number of transmit antenna at the BS, $\emptyset$: Azimuth angle . The steering (b) vector models the phases of signals across the transmit antennas at the BS, which are aligned to focus energy in the desired transmission direction $\emptyset$. It accounts for the spatial direction and frequency, making beamforming possible.

Similarity, the IRS-to-user channel is also specified [37]:

$$v_q = g_2\, e^{-j2\pi f_q t_2} k \tag{8}$$

The equation (8) models the IRS-U channel by considering path loss g_2, phase delays, and the steering vector of IRS. It ensures that IRS aligns the signals reflected to the user (U) .

Where, $g_2 \in \mathbb{C}$: the path gain channel (IRS-U), β_2 and α_2 are the elevation and azimuth angles of the Angle of Depature (AoD), $t_2 \in \mathbb{R}^+$represented the path delay, g_2 is given by [24]:

$$g_2 = \frac{c}{4\pi f_q d_2} e^{\frac{-\tau d_2}{2}} \approx \frac{c}{4\pi f_q d_2} \tag{9}$$

d_2: The distance from IRS to user (U).

At the q^{th} subcarrier,the gain of array is described using the system model, according to Yan *et al.* [25]:

$$A = \left|v_q^T \Theta G_q w\right| = \left|g_1 g_2 e^{-j2\pi(t_1+t_2)f_q}\right| . \left|k^T \Theta k b^H w\right| \tag{10}$$

Equation (10) combined all the components – BS, RIS, and UE – to express the total array gain, describing the impact of beamforming and IRS optimization.

Beam split analysis

The impact of beam split and its resulting gain of array and loss analysis were performed on an IRS surface. From equation (10), at q^{th} subcarrier, the normalized gain of array of the IRS was given by:

$$A_{IRS} = \left|k^T \Theta k b^H\right|$$
$$A_{IRS} = \frac{1}{N_1 N_2}\left|\sum_{n_1=0}^{N_1-1}\sum_{n_2=0}^{N_2-1} e^{j\pi m[n_1(a_1+a_2)+n_2(\vartheta_1+\vartheta_2)]}\right| . e^{j\theta_\ell} \tag{11}$$

Where, $\ell = N_2 n_1 + n_2 + 1$, $a_1 = \sin\alpha_1\cos\beta_1$, $\vartheta_1 = \sin\alpha_1 \sin\beta_1$, $a_2 = \sin\alpha_2\cos\beta_2$,

$\vartheta_2 = \sin\alpha_2 \sin\beta_2$, $m = \frac{f_q}{f_c}$ the relative frequency . The IRS beamforming vector was calculated using the transmitted signal's

https://doi.org/10.1017/S1759078725101669 Published online by Cambridge University Press

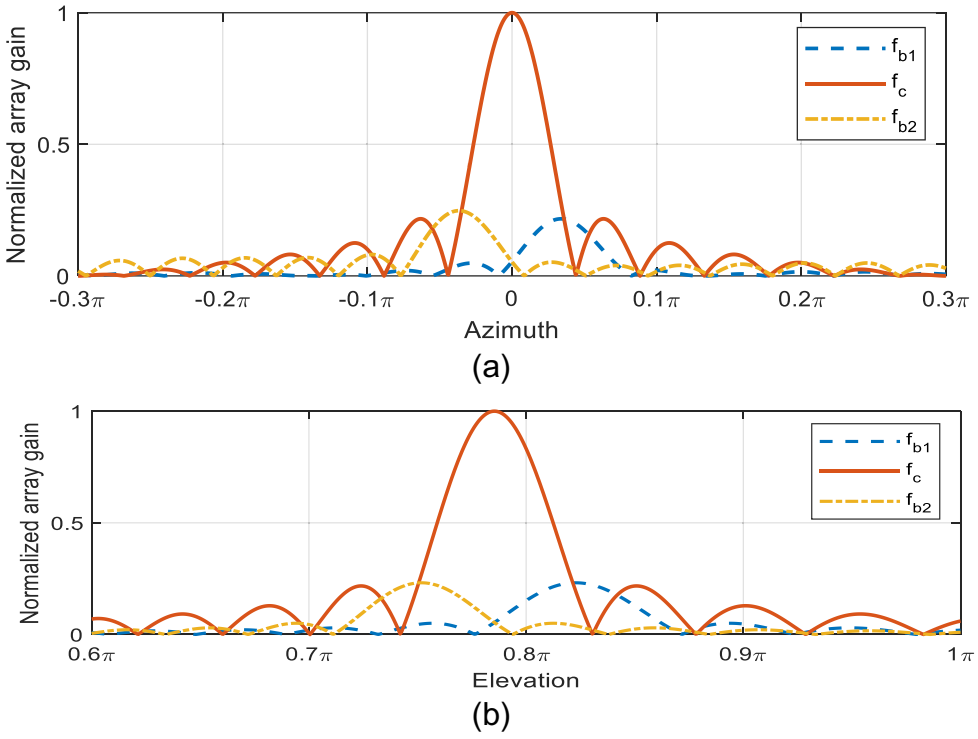


Figure 3. Array gain vs. (a) azimuth and (b) elevation angles.

carrier frequency as follow:

$$\theta_\ell = -\pi\left[n_1.\left(a_1 + a_2\right) + n_2.\left(\vartheta_1 + \vartheta_2\right)\right] \tag{12}$$

Let g_1 and g_2 remains constant, the normalized array gain (A_{IRS}) in equation (11) is written more succinctly as:

$$A_{IRS} = \frac{1}{N_1 N_2}\left|\sum_{n_1=0}^{N_1-1}\sum_{n_2=0}^{N_2-1} e^{j\pi(m-1)[n_1(a_1+a_2)+n_2(\vartheta_1+\vartheta_2)]}\right| \tag{13}$$

$$A_{IRS} \overset{(i)}{=} \mathbb{A}_{N_1}\left(\left(m-1\right)\left(a_1+a_2\right)\right)\mathbb{A}_{N_2}\left(\left(m-1\right)\left(\vartheta_1+\vartheta_2\right)\right) \tag{14}$$

Where (i) comes from $\sum_{n=0}^{N-1} e^{jn\pi x} = \frac{\sin\frac{N\in x}{2}}{\sin\frac{N\pi}{2}} e^{\frac{-j\pi(N-1)x}{2}}$ and $\mathbb{A}_N = \frac{sin\frac{N\pi x}{2}}{Nsin\frac{\pi x}{2}}$ is the Dirichlet Sinc Function [36].

Although the beam-splitting effect, caused by the intersection of a high number of IRS elements and broad bandwidth in mm-wave communications, is a significant problem resulting in a decrease in array gain, it is a challenge that spoils the potential advantage of IRS technology. To counter this issue, a wideband precoding method which modifies phase and delay simultaneously is introduced.

Design of irs structure

In this paper, a sub-connected PTDP architecture for IRS was proposed, replacing the conventional architecture depicted in Fig. 2a, for device cost saving. Frequency-selective precoding supported by the use of time delay units for every element in the IRS architecture in Fig. 2(b) [12, 36] effectively solves the beam splitting problem.Time delay units are power consuming and costly to accomplish compared to phase shifing. The sub-connected delay-phase architecture used in the Ref [36]. for BSs can't be extended directly to IRS, as destructive interference would occur due to the common TD unit. The considered structure, Fig. 2c utilizes two phase shifters per sub-array element that are linked by a shared TD unit via a circulator. A significant superposition of the signals is achieved by the main phase shifter layer of the subarray. Then, the time delay model shifts the signals timing, and the second phase shifter layer directs the resultant beam towards the required direction. The of proposed IRS structure is constructed with the help of two small antenna patches, each consisting of two layers of phase shifting. Compared to conventional time delay modules, the application of low-resolution phase shifters allows for significant power saving and hardware cost reduction. Furthermore, low-resolution components can be used by the integrated phase shifters to save power and reduce costs [38].

For the IRS-assisted mm-wave technology, it was assumed that the IRS is divided into $S = S_1S_2$ sub-arrays, where every sub-array is linked to a TD unit. Each sub-array include $P = P_1P_2$ elements, where $P_1 = N_1/S_1$ and $P_2 = N_2/S_2$. P_1 and P_2 values were converted into integers. Subarray parameters are set as $s_1 = 1, 2, \ldots, S_1$, and $s_2 = 1, \ldots, S_2$. The parameters of the elements in the individual subarray are taken as follows: $p_1 = 1, \ldots, P_1$, and $p_2 = 1, \ldots, P_2$.

Following structural modifications and subarray division, channel equations (3) and (8) are rewritten as the BS-IRS channel model introduced by the following equation:

$$G_q = \frac{g_1}{\sqrt{N_1N_2}} e^{-j2\pi f_q t_1} \underbrace{e^{j\pi m(n_1 a + n_2\vartheta}}_{steering\ matrix} \tag{15}$$

The channel of IRS-U is:

$$v_q = \frac{g_2}{\sqrt{N_1N_2}}\, e^{-j2\pi f_q t_2} e^{j\pi m(n_1 a + n_2\vartheta)} \tag{16}$$

Where $a = sin\alpha cos\beta$, $\vartheta = sin\alpha sin\beta$, $n_1 = s_1P_1 + p_1$, $n_2 = s_2P_2 + p_2$

https://doi.org/10.1017/S1759078725101669 Published online by Cambridge University Press

As seen in the equations (15) and (16), the channels G_q and v_q are divided into subarrays. G_q^s denoted the channel of the IRS subarray. The TD is $t_s \in \mathbb{R}^+$, Θ_1^s the first layer phase shift, Θ_2^s the second layer phase shift associated with sth subarray, and $s = s_2S_1 + s_1 + 1$. The vector of TD (T_q) of the elemnts of IRS is given by Dal *et al.* [20]:

$$\mathrm{T}_q = e^{-j2\pi f_q t},\ t = [t_1, t_2, \ldots., t_s, t_S] \tag{17}$$

Hence, the signal through the first phase-shifting layer of the sth IRS subarray is written as

$$\mathcal{Y}_{1,q}^s = \sum_{q=1}^{Q} \Theta_1^s \odot G_q^s \tag{18}$$

After going through the second phase-shifting layer, the user receives the signal:

$$\mathcal{Y}_{2,q}^s = \sum_{q=1}^{Q} \left(v_q^s \odot \Theta_2^s \mathrm{T}_q^s \mathcal{Y}_{1,q}^s\right) \tag{19}$$

Introducing phase shifts at two different stages allows for better control of the direction and timing of the reflected signals. A TD vector (T_q^s) is applied to ensure that across the subcarriers, alignment in the time domain improves to mitigate the beam split effects. Equations (18) and (19) are applied to obtain the gain of the q^{th} subarray of the IRS at the qth subcarrier:

$$A_s = \left| \sum_{q=1}^{Q} \left(v_q^s \odot \left[\Theta_2^s \mathrm{T}_q^s . \sum_{q=1}^{Q} \left(\Theta_1^s \odot G_q^s \right) \right] \right) \right| \tag{20}$$

Equation (20) shows that if time delays and phase shifts are added as proposed design parameters, it leads to achieving high array gains across different subcarriers of the proposed PTDP design, which in turn leads to mitigating the beam splitting effect.

PTDP-based IRS performance was quantified in terms of observing array gain. For solving beam splitting, a wideband precoding scheme was designed. The array gain for the q^{th} subcarrier was determined via equation (20):

$$A = \left| \sum_{s_1=1}^{S_1} \sum_{s_2=1}^{S_2} \left\{ \sum_{q=1}^{Q} \left(v_q^s \odot \left[\Theta_2^s \mathrm{T}_q^s . \sum_{q=1}^{Q} \left(\Theta_1^s \odot G_q^s \right) \right] \right) \right\} \right| \tag{21}$$

The optimization problem for maximizing the array gain over all subcarriers is:

$$\frac{\max}{\Theta_1, \Theta_2, t} \frac{1}{Q} \sum_{q=1}^{Q} A \tag{22}$$

Wideband precoding performance gains at the qth subcarrier for PTDP-based are conditioned on (23) to (25).

$$t_s = \frac{1}{2f_c} \left[\left((s_1 - 1) P_1 - \frac{(P_1 - 1)}{2} \right) (a_1 + a_2) + \left((s_2 - 1) P_2 - \frac{(P_2 - 1)}{2} \right) (\vartheta_1 + \vartheta_2) \right] \tag{23}$$

$$\Theta_1^s = e^{-j\pi(p_1 a_1 + p_2 \vartheta_1)} \tag{24}$$

$$\Theta_2^s = e^{-j\pi(p_1 a_2 + p_2 \vartheta_2)} \tag{25}$$

The equation (23) shows that the optimal time delay depends on the size of the sub-array (parameters $P_1$and P_2) and the angular parameters a and ϑ related to the signal direction. Properly introducing time delays compensates for frequency-dependent beam misalignment. As equation (18) is a scalar value, the maximization of equation (22) is equivalent to the maximization of equations (18) and (19) individually.

The array gain of the proposed PTDP was subsequently defined, having been determined through the resolution of the equation (21) [20]:

$$A = \frac{S_1 S_2 P_1 P_2}{N_1 N_2} \left| \mathbb{A}_{P_1} \left((m-1) a_1 \right) \mathbb{A}_{P_1} \left((m-1) a_2 \right) . \mathbb{A}_{P_1} \left((m-1) \vartheta_1 \right) \mathbb{A}_{P_1} \left((m-1) \vartheta_2 \right) \right| \tag{26}$$

The stages involved in PTDP beamforming are illustrated in Algorithm 1. Ideal Phase Shift differs from PTDP Phase Shift in that the ideal was calculated directly from the IRS element's frequency and index. The second one, contains a delay component adjusted in order to offset sub-arrays and sub-array layers' phase shifts. According to equation (12), the IRS's optimal beamforming vector ought to be frequency-dependent [16]:

$$\theta_{opt,\ell} = -\pi m \left[n_1 . (a_1 + a_2) + n_2 . (\vartheta_1 + \vartheta_2) \right] \tag{27}$$

The proposed PTDP architecture for IRS has transformative practical implications in several scenarios, including:

Algorithm 1: The proposed PTDP beamforming

Input: The angles values (α_1),(β_1) ,(α_2) and (β_2) of the IRS.

Initialization:

1. Calculate $a_1 = sin\alpha_1 cos\beta_1$, $\vartheta_1 = sin\alpha_1 sin\beta_1$, $a_2 = sin\alpha_2 cos\beta_2$, $\vartheta_2 = sin\alpha_2 sin\beta_2$.
2. Calculate optimal time delay from equation (23)
3. Calculate the phase shifts of subarrays from equations (24) and (25)

Output: The normalized array gain from equation (26).

1. High-Speed Wireless Networks: Beamforming and signal alignment can be improved for 5G/6G mm-wave communication to increase reliability and throughput.
2. Dense Urban Areas: Path loss and interference are minimized in dense areas, providing stable IRS assisted connections.
3. Autonomous Systems: Provides precise beam steering for real-time data transfer in autonomous vehicles and drones, providing low latency in communication.
4. Industrial IoT and Smart Manufacturing: It improves communication within IoT networks by enhancing the quality of the signal to facilitate automation in industries effectively.

There are essential differences between the proposed PTDP and Ref. [25]:

Difference in operating mode and functionality: In [25], the STAR-RIS system is used for joint reflection and transmission control, introducing additional challenges in the wideband beamforming design from the aspect of managing three-sided beam splitting. Our contribution is devoted to the conventional reflection-only IRS scenario in order to empower sophisticated precoding schemes for the mm-wave scenario.

Impact of side structure on system performance: As mentioned by the reviewer, our paper's RIS structure is a special case of STAR-RIS in [25], but it ignores the geometrical and radiation implications of having two separate surfaces in STAR-RIS versus one surface in conventional RIS. This difference leads to varying mathematical formulations and optimization methods, and thus the two approaches are not equivalent in performance and computational complexity.

https://doi.org/10.1017/S1759078725101669 Published online by Cambridge University Press

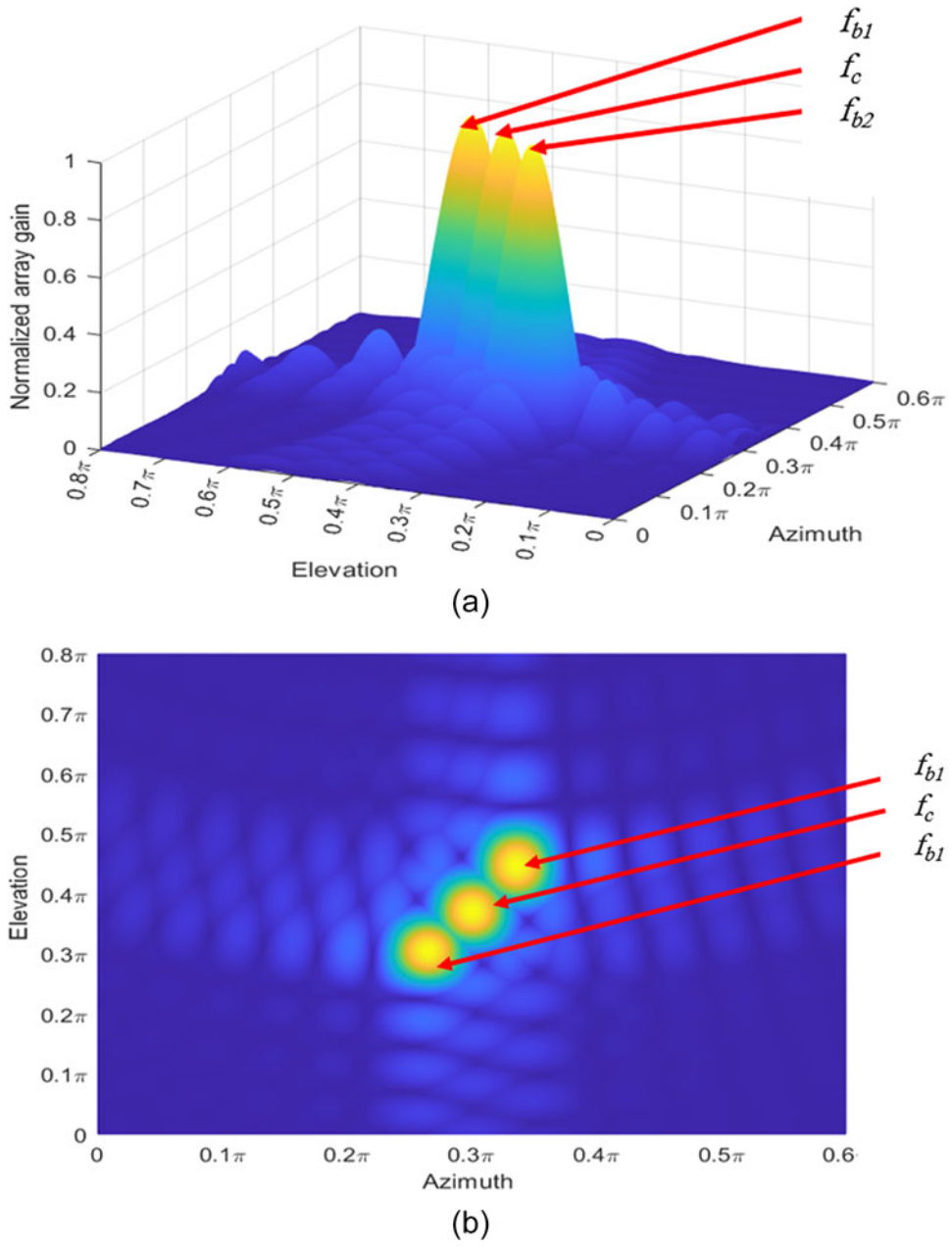


Figure 4. Beam splitting at IRS. (a) 3-dimension view (b) an overview from above.

Research focus and explicit applications: The present research attempts to provide customized solutions for conventional IRS configurations in mm-wave communication systems with proficiency in Wideband Precoding techniques, whose mathematical formulations and analyses differ from what is used in STAR-RIS.

Therefore, structural similarity is not equal to similar modeling, analysis, and applications because the diversity of the research goals and theory makes up the different approach that suits a different set of real-world situations.

Simulation results

The simulation of an IRS-aided mm-wave communication system, presented in Sections 3 and 4 and illustrated graphically in Fig. 1, was conducted with the parameters listed in Table 1. It is assumed that the channel state information CSI is perfectly available [9], obtained using the techniques in [10, 11].

The elevation and azimuth angles were fixed, which present the certain physical directions that result in the maximum array gain. Figure 3a and b illustrates the independent relationships between azimuth angle, elevation angle, and array gain. A reference received beam at the center frequency f_c was used, and compared with the received beam at the other frequencies (f_{b_1} and f_{b_2}). The boundary of the band beams was found to be severely displaced from the desired direction. In addition, the 3D view in Fig. 4(a) clearly highlights the splitting of the three beams into different directions. Figure 4b shows that the three beams were successfully separated according to the variables of elevation and azimuth angles, as planned.

Figure 5 illustrates the relationship between array gain and subcarrier frequency. As more frequencies are used, the array gain is

https://doi.org/10.1017/S1759078725101669 Published online by Cambridge University Press

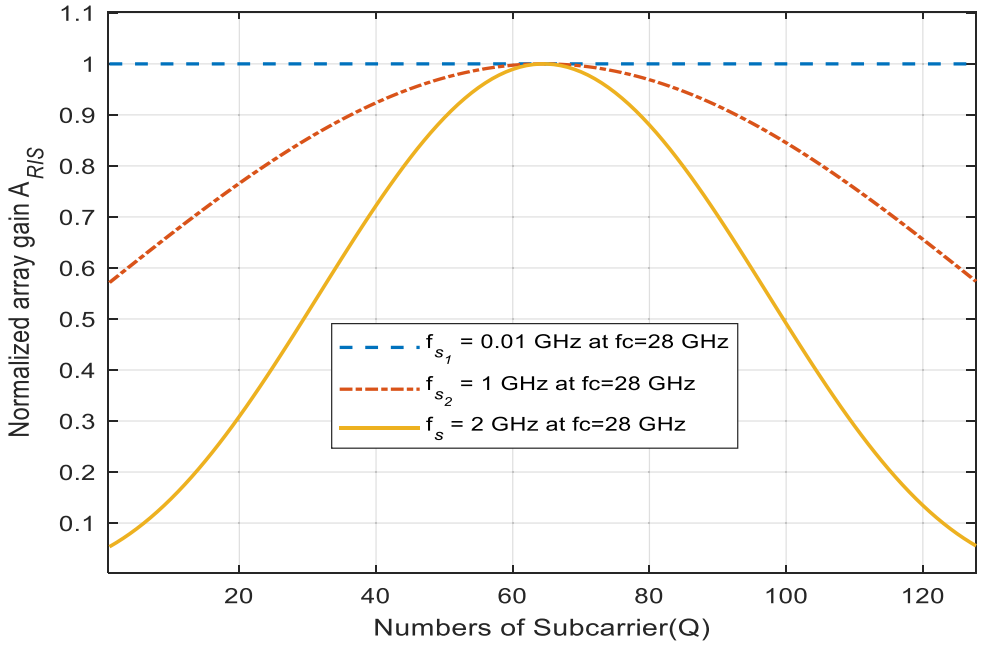


Figure 5. Array gain vs. the sub-carrier number for the bandwidths $f_{s1} = 0.01\ GHz,\ f_{s1} = 1\ GHz,\ and\ f_{s1} = 2\ GHz$..

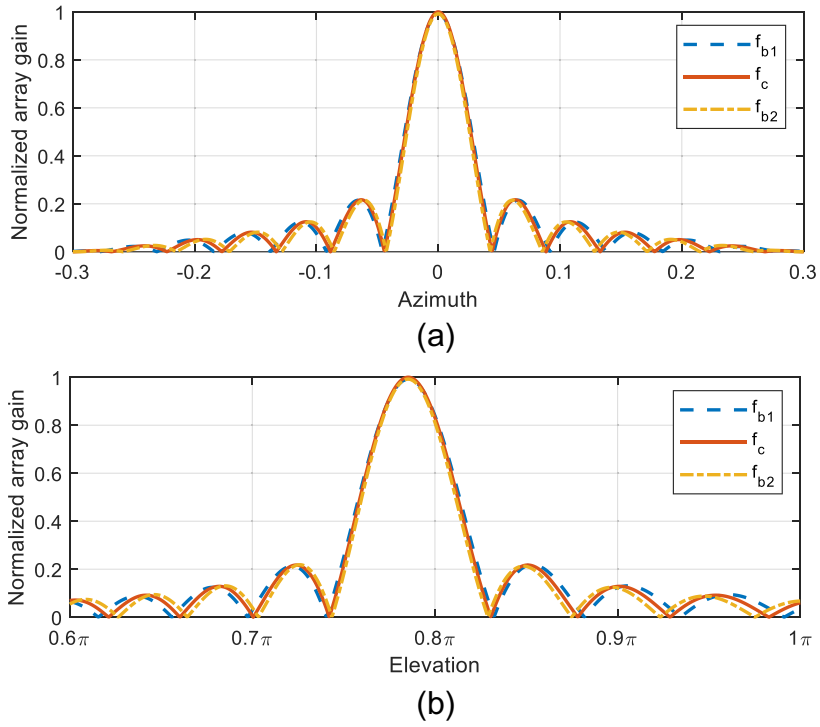


Figure 6. Array gain (A) vs (a) azimuth angle and (b) elevation angle for proposed PTDP architecture.

lost. Consequently, having a large bandwidth increase causes an extensive loss in gain, thus decreasing the advantage of employing IRS technology.

The suggested PTDP system can steer beams produced at different frequencies correctly, as evident from Figs. 6 and 7. The suggested method significantly improves beam alignment to target angles in comparison to the old system with massive gain reduction. This demonstrates that the phase shifters and TD units utilized in the proposed system operate effectively.

Figure 8 illustrates the normalized array gain versus multiple subcarriers. A comparison of Fig. 8 and Fig. 5 shows that the proposed PTDP and wideband precoding structure effectively eliminates the beam-splitting effect. Specifically, the normalized reduction in array gain is over 82% at subcarrier $Q = 1$ when used with a narrowband frequency . The results in Fig. 8 show how effective the proposed PTDP design is in solving the beam-splitting issue in IRS systems. The comparison between the performance of the proposed system and the traditional beamforming system

https://doi.org/10.1017/S1759078725101669 Published online by Cambridge University Press

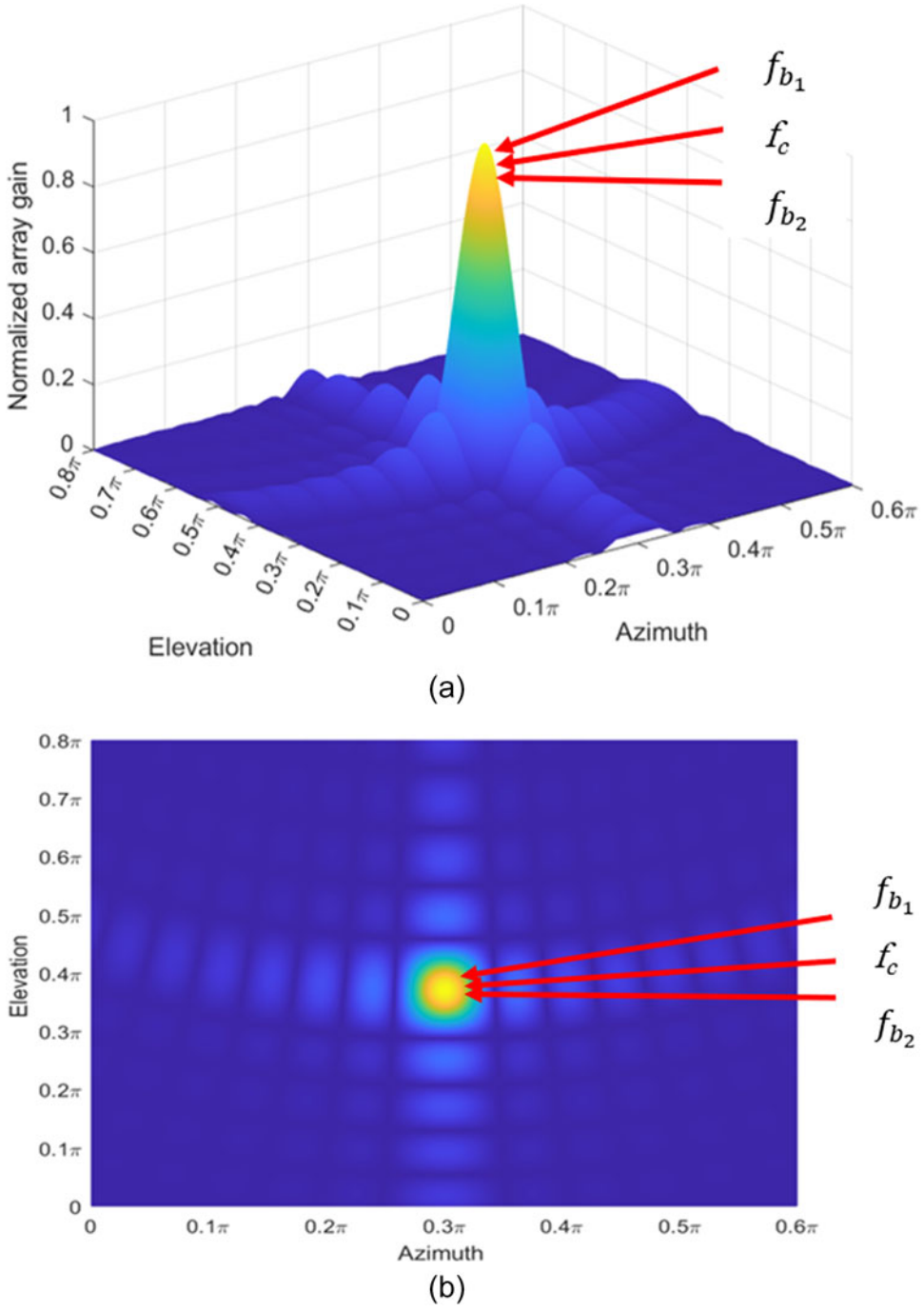


Figure 7. Beams generated using PTDP method:(a) 3D view (b) a bird's-eye perspective.

for various frequency bands reveals the proposed design provides much greater array gain, particularly in wideband scenarios. The new design improved the gain by 94.5% in comparison to the traditional approach.

Figure 9 demonstrates the relation between the rate of each subcarrier and the BS's transmitted power. When every element in the suggested system has a time delay, its frequency-based precoding architecture can reach the best performance. The architecture was based on conventional narrowband beamforming and focused on enhancing phase control performance, which was compared with the conventional design using continuous phase shifting and low-resolution phase shifting (1 and 2 bits) and with the conventional method. The proposed design in this work was also optimized to the best precoding. Conventional narrowband beamforming has been designed using basic phase shift. The proposed PTDP is designed on advanced phase shifting, and considerable performance gain is obtained using these shifts.The result concluded that the data rate is enhanced by 54% at a transmitted power of 30 dBm when the proposed design is employed compared to the conventional design.

https://doi.org/10.1017/S1759078725101669 Published online by Cambridge University Press

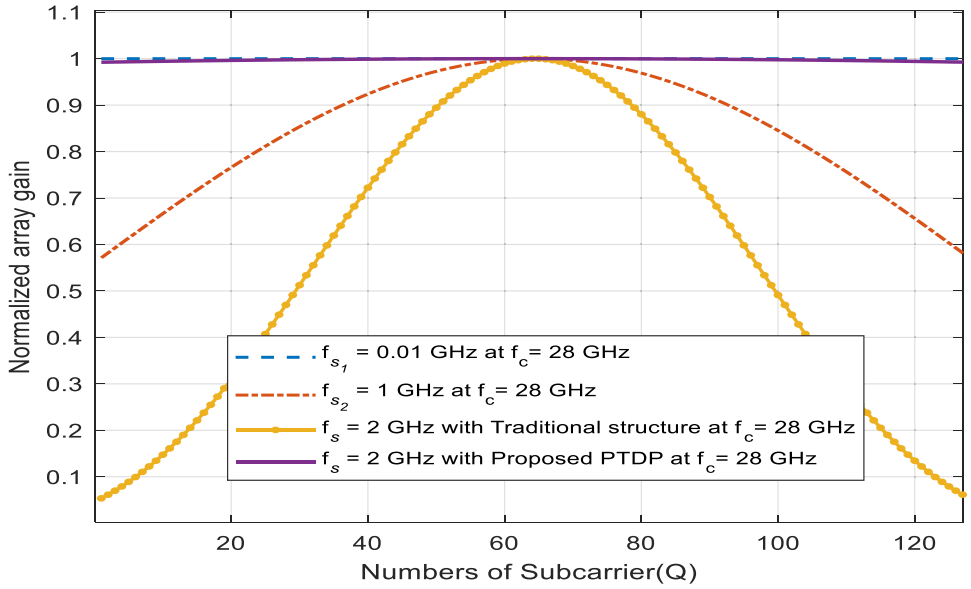


Figure 8. The relationship between normalized array gain and number of sub-carriers using proposed PTDP structure.

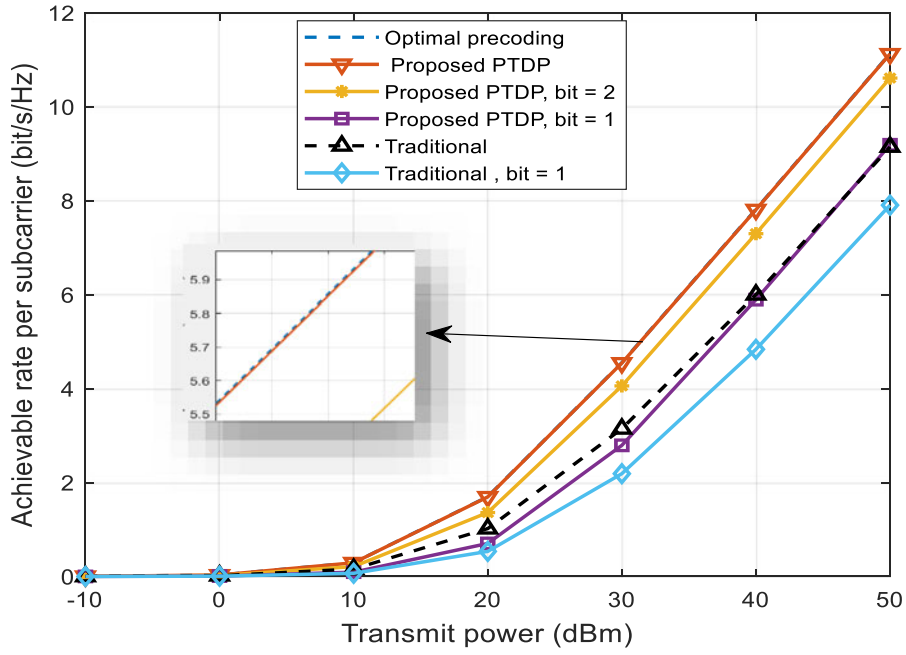


Figure 9. Transmitted power vs achievable rate per subcarrier.

The achievable rate for each subcarrier is defined as [39, 40]:

$$R_{optimal} = \frac{1}{Q}\sum_{q=1}^{Q} log_2\left(1 + \frac{|G_q|^2.SNR}{\sigma^2}\right) \quad (30)$$

Where the Signal-to-Noise Ratio (SNR):

$$SNR = \frac{P_t}{\sigma^2} \quad (31)$$

Where the total transmitted power denoted P_t, and $\sigma^2 = -90dBm$ [9, 41].

The continuous precoding achievable rate is expressed as:

$$R_{con} = \frac{1}{Q}\sum_{q=1}^{Q} log_2\left(1 + \frac{|\Theta_1 G_q \Theta_2|^2 SNR}{\sigma^2}\right) \quad (32)$$

Figure 10 illustrates that with an increase in the number of subarrays, the rate per subcarrier also increases, and as it rises its value is also nearer to ideal precoding. Figure 11 explain the relation between Energy Efficiency and transmited power. Optimal Precoding represents the best possible performance in terms of energy efficiency at different levels of transmission power. The proposed method Proposed PTDP shows a performance close to the optimal but with some differences.

Proposed PTDP with 1-bit, 2-bi refers to the use of a limited-precision digital representation (1-bit, 2-bit) in signal processing. The more bits, the better the performance due to the increased precision of the representation. Traditional and Traditional 1-bi represent the traditional methods with and without using a limited-precision representation. They are usually less efficient

https://doi.org/10.1017/S1759078725101669 Published online by Cambridge University Press

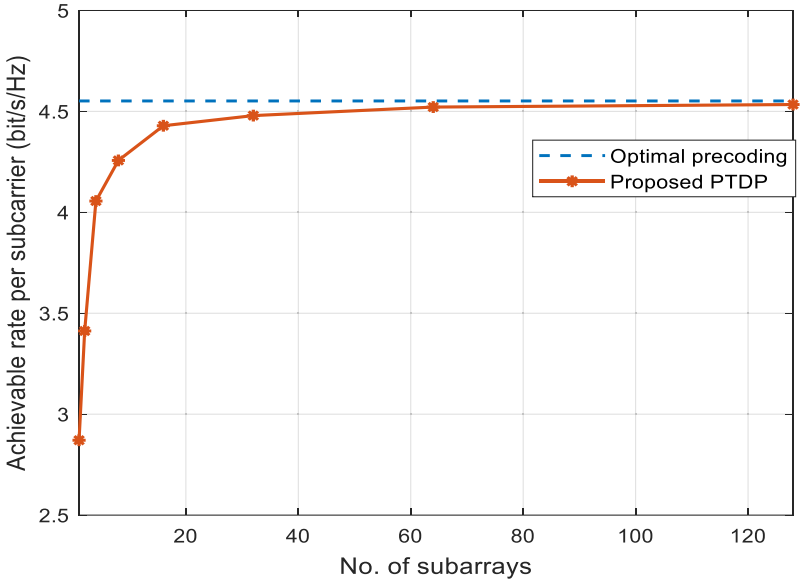


Figure 10. The number of subarrays vs. The achievable rate.

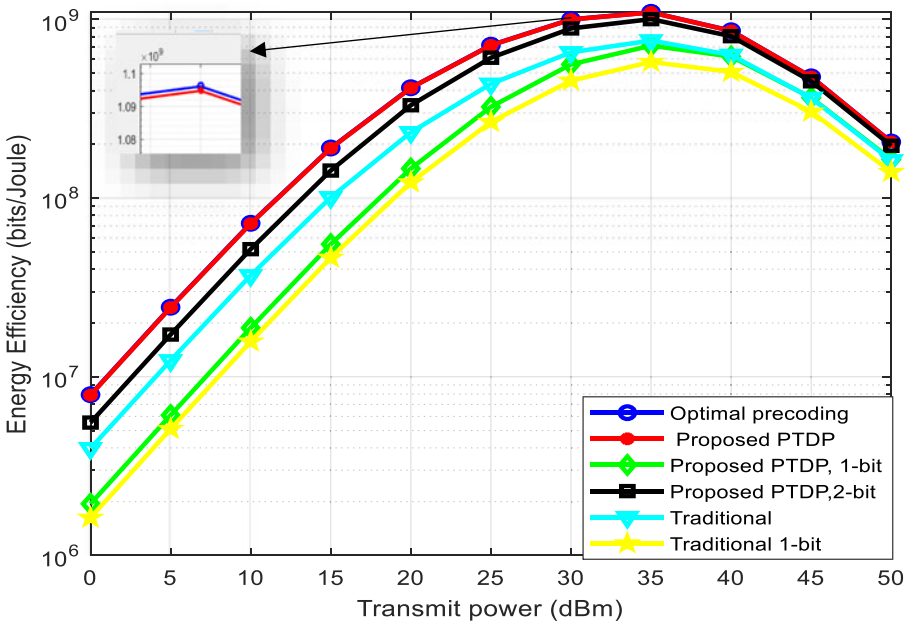


Figure 11. Energy efficiency (bits/joule) vs transmitted power(dbm).

than the proposed methods. As the transmited power increases, the energy efficiency of all methods improves due to the improved signal quality. The proposed methods (Proposed PTDP) outperform the traditional methods, especially when using a higher-precision representation (2-bit). Using a limited-precision representation (1-bit) reduces the energy efficiency compared to the higher-precision representation, but it may be beneficial in reducing the computational complexity and energy consumption. It is clear from this that the results show that the proposed methods, especially with increasing representation accuracy, provide better energy efficiency compared to conventional methods, and that increasing transmission power leads to an improvement in overall energy efficiency. Figure 12 shows the relationship between energy efficiency and SNR for different precoding schemes in wireless communication systems. Energy efficiency is measured in bits/joule, which indicates the number of bits that can be transmitted using one joule of energy. Optimal precoding shows the highest energy efficiency across all SNR values, indicating that it is the most energy efficient. The proposed PTDP scheme shows good performance and efficiency close to optimal precoding. The 1-bit and 2-bit PTDP schemes show lower energy efficiency compared to the proposed scheme, indicating that reducing the encoding accuracy negatively affects the efficiency.

The traditional scheme shows the lowest energy efficiency, indicating that it is less energy efficient compared to the other schemes.

The energy efficiency was given in below [42]:

$$\text{Energy Efficiency } (EE) = \frac{BW.R}{Total\ power} \tag{33}$$

Where $Total\ power = P_{static} + P_{IRS} + v^{-1}P_{transmit}$ [42], $P_{static} = 4watt$, $P_{IRS} = N_1N_2P_n$, the element power consumption is $P_n = 1mw$, $v^{-1} = 1$ [43], and $P_{transmit} = 0$ to 50 dBm.

https://doi.org/10.1017/S1759078725101669 Published online by Cambridge University Press

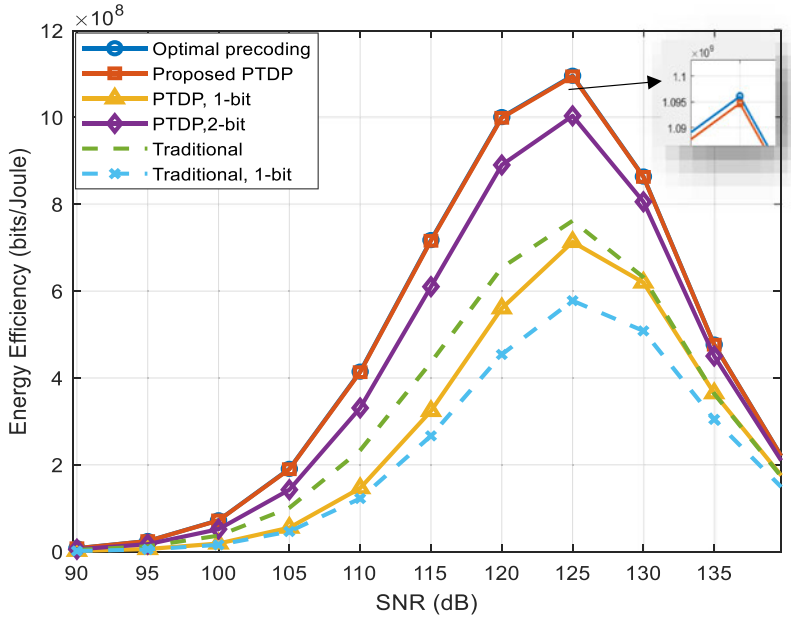


Figure 12. Energy efficiency (bits/joule) vs SNR (db).

Conclusion

Millimeter wave communication aided by IRS has been faced with the challenge of beam splitting, which results in received signal power loss. In order to combat this problem, phase shift and time delay-based signal precoding schemes have been explored. Building on the beam splitting effect analysis and gain loss analysis, the IRS structure composed of multiple connected layers is proposed. This setup enables the application of a frequency-based and error-tolerant precoding approach for communication channel estimation. The results demonstrate that this approach effectively mitigates the impact of beam splitting, enhancing the efficiency of IRS-assisted mm-wave technology. The proposed PTDP accomplished 94.5% gain improvement over the traditional architecture. In general, it is observed that energy efficiency improves with increasing SNR, but the rate of improvement varies between schemes. The optimal scheme shows the best performance, while the traditional scheme shows the lowest performance. This points out the importance of selecting appropriate precoding schemes to improve the energy efficiency of wireless communication systems.

Competing interest. The authors declare that they have no competing financial interests or personal relationships known to them that could have appeared to influence the work reported in this paper.

References

1. **Roberts IP, Zhang Y, Osman T and Alkhateeb A** Real-World Evaluation of Full-Duplex Millimeter Wave Communication Systems. *IEEE Transactions on Wireless Communications*, 2024.
2. **Ahmad BM, Mahmood FE, and Alsawaf HA** (2023) Non Orthogonal Multiple Access verses Orthogonal Multiple Access performance comparison in 5G communication systems. *Przeglad Elektrotechniczny* **99**, 129. doi:10.15199/48.2023.01.25.
3. **Abed RA and Ayoob SA**. Millimeter wave beams coordination and antenna array height effect. In *AIP Conference Proceedings*, 2023.
4. **Qeryaqos BJ and Ayoob SA** (2024) Optimizing the signal-to-noise ratio using the virtual line of sight and choosing the appropriate dimensions. *International Journal of Electronics and Telecommunication* **70**, 909–914. doi:10.24425/ijet.2024.152077.
5. **Qeryaqos BJ and Ayoob SA** (2025) Improving SINR with smart RIS solutions: Exploring optimal dimensions and sizes. *International Journal of Microwave and Wireless Technologies* **17**, 1–10. doi:10.1017/S1759078725000169.
6. **Wu Q and Zhang R** (2019) Towards smart and reconfigurable environment: Intelligent reflecting surface aided wireless network. *IEEE Communications Magazine* **58**, 106–112. doi:10.1109/MCOM.001.1900107.
7. **Li R, Guo B, Tao M, Liu Y-F and Yu W** (2022) Joint design of hybrid beamforming and reflection coefficients in RIS-aided mmWave MIMO systems. *IEEE Transactions on Communications* **70**, 2404–2416. doi:10.1109/TCOMM.2022.3144986.
8. **Zhang Z and Dai L** (2021) A joint precoding framework for wideband reconfigurable intelligent surface-aided cell-free network. *IEEE Transactions on Signal Processing* **69**, 4085–4101. doi:10.1109/TSP.2021.3088755.
9. **Wang P, Fang J, Yuan X, Chen Z and Li H** (2020) Intelligent reflecting surface-assisted millimeter wave communications: Joint active and passive precoding design. *IEEE Transactions on Vehicular Technology* **69**, 14960–14973. doi:10.1109/TVT.2020.3031657.
10. **Ma S, Shen W, An J and Hanzo L** (2021) Wideband channel estimation for IRS-aided systems in the face of beam squint. *IEEE Transactions on Wireless Communications* **20**, 6240–6253. doi:10.1109/TWC.2021.3072694.
11. **Hu C, Dai L, Han S and Wang X** (2021) Two-timescale channel estimation for reconfigurable intelligent surface aided wireless communications. *IEEE Transactions on Communications* **69**, 7736–7747. doi:10.1109/TCOMM.2021.3072729.
12. **Liu K, Zhang Z, Dai L, Xu S and Yang F** (2021) Active reconfigurable intelligent surface: Fully-connected or sub-connected? *IEEE Communications Letters* **26**, 167–171. doi:10.1109/LCOMM.2021.3119696.
13. **Pan C, Ren H, Wang K, Xu W, Elkashlan M, Nallanathan A and Hanzo L** (2020) Multicell MIMO communications relying on intelligent reflecting surfaces. *IEEE Transactions on Wireless Communications* **19**, 5218–5233. doi:10.1109/TWC.2020.2990766.
14. **He M, Xu W, Shen H, Xie G, Zhao C and Di Renzo M** (2021) Cooperative multi-RIS communications for wideband mmWave MISO-OFDM systems. *IEEE Wireless Communications Letters* **10**, 2360–2364. doi:10.1109/LWC.2021.3100479.
15. **Wang P, Fang J, Zhang W and Li H** (2021) Fast beam training and alignment for IRS-assisted millimeter wave/terahertz systems. *IEEE Transactions on Wireless Communications* **21**, 2710–2724. doi:10.1109/TWC.2021.3115152.

16. **Chen Y, Chen D and Jiang T**, "Beam-squint mitigating in reconfigurable intelligent surface aided wideband mmWave communications," in *2021 IEEE Wireless Communications and Networking Conference (WCNC)*, 2021, 1–6.
17. **Nuti P, Balti E and Evans BL** Spectral efficiency optimization for mmWave wideband MIMO RIS-assisted communication. in *2022 IEEE 95th Vehicular Technology Conference:(VTC2022-Spring)*, 2022, 1–6.
18. **Wang R, Yang Y, Makki B and Shamim A** A wideband reconfigurable intelligent surface for 5G millimeter-wave applications. *IEEE transactions on antennas and propagation*, 2024.
19. **Zhao Y, Liu X, Liu H, Wang X, and Huang L** (2024) RIS-Aided MmWave hybrid relay network based on multi-agent deep reinforcement learning. *Mobile Networks and Applications* **29**, 825–840. doi:10.1007/s11036-024-02323-x.
20. **Dai L, Tan J, Chen Z and Poor HV** (2022) Delay-phase precoding for wideband THz massive MIMO. *IEEE Transactions on Wireless Communications* **21**, 7271–7286. doi:10.1109/TWC.2022.3157315.
21. **Chen Y, Xiong Y, Chen D, Jiang T, Ng SX and Hanzo L** (2020) Hybrid precoding for wideband millimeter wave MIMO systems in the face of beam squint. *IEEE Transactions on Wireless Communications* **20**, 1847–1860. doi:10.1109/TWC.2020.3036945.
22. **An J, Xu C, Ng DWK, Yuen C, Gan L and Hanzo L** Reconfigurable intelligent surface-enhanced OFDM communications via delay adjustable metasurface. *arXiv preprint arXiv:2110.09291*, 2021.
23. **Park S-H, Kim B, Kim DK, Dai L, Wong -K-K and Chae C-B** (2022) Beam squint in ultra-wideband mmWave systems: RF lens array vs. phase-shifter-based array. *IEEE Wireless Communications* **30**, 82–89. doi:10.1109/MWC.007.2100530.
24. **Li R, Shao X, Sun S, Tao M and Zhang R** IRS aided millimeter-wave sensing and communication: beam scanning, beam splitting, and performance analysis. *arXiv preprint arXiv:2401.15344*, 2024.
25. **Yan W, Hao W, Sun G, Huang C and Wu Q** Wideband beamforming for Star-RIS-assisted THZ communications with three-side beam split *IEEE Transactions on Communications*, 2024.
26. **Alsawaf HA and Ayoob SA** (2025) Compressive Channel Estimation for Hybrid Passive/Active IRS-Assisted mm-Wave MIMO Systems. *Journal of Communications* **20**, 166–175. doi:10.12720/jcm.20.2.166-175.
27. **Torcolacci G, Guerra A, Zhang H, Guidi F, Yang Q, Eldar YC and Dardari D**, Holographic imaging with XL-MIMO and RIS: Illumination and reflection design. in *IEEE Journal of Selected Topics in Signal Processing*, 2024.
28. **Xiu Y, Zhao J, Sun W, Renzo MD, Gui G, Zhang Z and Wei N** (2021) Reconfigurable intelligent surfaces aided mmWave NOMA: Joint power allocation, phase shifts, and hybrid beamforming optimization. *IEEE Transactions on Wireless Communications* **20**, 8393–8409. doi:10.1109/TWC.2021.3092597.
29. **Qeryaqos BJ and Ayoob SA** (2024) Proposed multiple reconfigurable intelligent surfaces to mitigate the inter-user-interference problem in NLOS. *Journal of Communications Software and Systems* **20**, 245–252. doi:10.24138/jcomss-2024-0039.
30. **Ning B, Chen Z, Chen W, Du Y and Fang J** (2021) Terahertz multi-user massive MIMO with intelligent reflecting surface: Beam training and hybrid beamforming. *IEEE Transactions on Vehicular Technology* **70**, 1376–1393. doi:10.1109/TVT.2021.3052074.
31. **Liu Y, Zhang S, Gao F, Tang J and Dobre OA** (2021) Cascaded channel estimation for RIS assisted mmWave MIMO transmissions. *IEEE Wireless Communications Letters* **10**, 2065–2069. doi:10.1109/LWC.2021.3092147.
32. **Mei W and Zhang R** (2021) Multi-beam multi-hop routing for intelligent reflecting surfaces aided massive MIMO. *IEEE Transactions on Wireless Communications* **21**, 1897–1912. doi:10.1109/TWC.2021.3108020.
33. **Li R, Sun S and Tao M** (2022) Ergodic achievable rate maximization of RIS-assisted millimeter-wave MIMO-OFDM communication systems. *IEEE Transactions on Wireless Communications* **22**, 2171–2184. doi:10.1109/TWC.2022.3210227.
34. **Ling T, Han Y, Jin S and Matthaiou M** Two-phase parameter-based separate channel estimation in RIS-Aided MIMO OFDM systems. in *ICC 2023-IEEE International Conference on Communications*, 2023, 4329–4334.
35. **Pei X, Yin H, Tan L, Cao L, Li Z, Wang K, Zhang K and Björnson E** (2021) RIS-aided wireless communications: Prototyping, adaptive beamforming, and indoor/outdoor field trials. *IEEE Transactions on Communications* **69**, 8627–8640. doi:10.1109/TCOMM.2021.3116151.
36. **Tan J and Dai L** Delay-phase precoding for THz massive MIMO with beam split. in *2019 IEEE Global Communications Conference (GLOBECOM)*, 2019, 1–6.
37. **Wei Y, Zhao -M-M, Zhao M-J and Cai Y** (2021) Channel estimation for IRS-aided multiuser communications with reduced error propagation. *IEEE Transactions on Wireless Communications* **21**, 2725–2741. doi:10.1109/TWC.2021.3115161.
38. **Huang C, Alexandropoulos GC, Zappone A, Debbah M and Yuen C** Energy efficient multi-user MISO communication using low resolution large intelligent surfaces in *2018 IEEE Globecom Workshops (GC Wkshps)*, 2018, 1–6.
39. **Cheng Y, Huang C, Peng W, Debbah M, Hanzo L and Yuen C** Achievable rate optimization of the RIS-aided near-field wideband uplink, *IEEE Transactions on Wireless Communications*, 2023.
40. **Wang J, Xiao J, Zou Y, Xie W and Liu Y** Wideband Beamforming for RIS Assisted Near-Field Communications. *arXiv preprint arXiv:2401.11141*, 2024.
41. **Yang S, Xie C, Lyu W, Ning B, Zhang Z and Yuen C** Near-field channel estimation for extremely large-scale reconfigurable intelligent surface (XL-RIS)-aided wideband mmwave systems *IEEE Journal on Selected Areas in Communications*, 2024.
42. **Huang C, Zappone A, Alexandropoulos GC, Debbah M and Yuen C** (2019) Reconfigurable intelligent surfaces for energy efficiency in wireless communication. *IEEE Transactions on Wireless Communications* **18**, 4157–4170. doi:10.1109/TWC.2019.2922609.
43. **Li Z, Zhang J, Zhu J, and Dai L** (2023) RIS energy efficiency optimization with practical power models. in *Proc. IEEE Int. Wireless Commun. Mobile Comput. Conf. (IWCMC), Jun. 2023*, 1172–1177. doi:10.1109/IWCMC58020.2023.10183034



Hiba A. Alsawaf Mrs. Hiba earned her B.E. in electrical engineering/electronic and communications engineering from the University of Mosul, Iraq. The same university also awarded her a master's degree in electronic and communication engineering and she is now working for a PhD in 6G communication. She has taught at Nineveh University's College of Electronics Engineering for 14 years. She can be contacted at email: hiba.hmdoon@uoninevah.edu.iq



Saad A. Ayoob was born in Ninevah Province, Iraq, in 1972. He received his B.S. degree from the University of Mosul, Iraq, in 1996 and his M.S. degree and Ph.D. from the same University in 2005 and 2011 respectively, both in Communication Engineering. He is currently an Assistant Prof. in the Department of Electrical Engineering, University of Mosul. His research interests include networking, millimeter-wave, 5G, 6G, microstrip patch antenna, Reconfigurable intelligent surfaces (RIS), and communication systems. He can be contacted at email: sa_ah_ay@uomosul.edu.iq

https://doi.org/10.1017/S1759078725101669 Published online by Cambridge University Press